Acta Crystallographica Section F
**Structural Biology and Crystallization Communications**
ISSN 1744-3091

# Crystallization and preliminary crystallographic analysis of the complex of the second and third regulatory subunits of human Pol δ

**Andrey G. Baranovskiy, Nigar D. Babayeva, Youri I. Pavlov and Tahir H. Tahirov***

Eppley Institute for Research in Cancer and Allied Diseases, University of Nebraska Medical Center, 986805 Nebraska Medical Center, Omaha, NE 68198-7696, USA

Correspondence e-mail: ttahirov@unmc.edu

Received 9 June 2008
Accepted 4 August 2008



Human DNA polymerase δ (Pol δ) consists of four subunits: p125, p50, p66 and p12. A heterodimer containing a His-tagged p50 subunit (p50) and a p50-interacting domain of the p66 subunit ($p66_N$) was crystallized. The crystal was in the form of a prism with a rhombic cross-section and belonged to space group $P2_1$. The crystal had unit-cell parameters $a$ = 95.13, $b$ = 248.54, $c$ = 103.46 Å, $\beta = 106.94^\circ$ and diffracted to a resolution of 3 Å. Four molecules of p50–$p66_N$ in an asymmetric unit corresponded to a crystal solvent content of 72.2%.

## 1. Introduction

Pol δ is one of three major replicases in eukaryotes (McCulloch & Kunkel, 2008). It also plays an essential role in translesion DNA synthesis, homologous recombination and DNA repair (Pavlov *et al.*, 2006). Human Pol δ consists of four subunits: p125, p50, p66 and p12 (Liu *et al.*, 2000; Podust *et al.*, 2002). The p125 subunit possesses exonuclease and DNA polymerase activities, while the remaining three subunits fulfill a regulatory role and stimulate the polymerase activity of p125 by mediating interactions with PCNA. They also stabilize the entire Pol δ complex. In the latter function, p50 serves as a scaffold for the assembly of Pol δ by interacting simultaneously with the other three subunits (Li, Xie, Zhou *et al.*, 2006). In addition, p50 is also involved in the recruitment of several Pol δ regulating proteins, including p21 (Li, Xie, Rahmeh *et al.*, 2006), PDIP1 (He *et al.*, 2001), PDIP38 (Liu *et al.*, 2003), PDIP46 (Liu *et al.*, 2003) and WRN (Szekely *et al.*, 2000). The fragments of p50 that are responsible for interaction with p66, p125 and p12 have not been defined. Using a two-hybrid screening, human p66 has been shown to contain p50-binding and PCNA-binding domains within the 144 N-terminal and 20 C-terminal amino acids, respectively (Pohler *et al.*, 2005). Studies with the model organism *Saccharomyces cerevisiae* (baker's yeast) revealed that many of the essential functions of Pol δ, including its involvement in break-induced replication (BIR; Lydeard *et al.*, 2007) and the mutagenic bypass pathway (Gerik *et al.*, 1998; Huang *et al.*, 2000, 2002; Gibbs *et al.*, 2005), depend on interactions between pol31 and pol32, which are the yeast orthologues of human p50 and p66, respectively. Interestingly, only the pol31-binding domain of pol32 (Johansson *et al.*, 2004) was essential and sufficient for the contribution of Pol δ to BIR (Lydeard *et al.*, 2007). In order to understand why the p50–p66 interactions are so important for the function of Pol δ, it would be useful to solve the three-dimensional structure of the p50–p66 heterodimer using X-ray crystallography. As a first step towards this goal, we report the crystallization of p50 in complex with the p50-interacting domain of p66.

## 2. Materials and methods

### 2.1. Cloning, expression and purification

The cDNAs for the p50 and p66 subunits of Pol δ were obtained from Open Biosystems (clone IDs 2822169 and 40010009, respectively). A full-length cDNA for the p66 subunit was made by adding 60 missing nucleotides at the 5′-terminus by two-step PCR with forward primers AGACGAGTTCGTCACGGACCAAAACAAG-

ATCGTGACATACAAATGGCTGAGC and CGCGGCTGGATCCTAAATATGGCGGACCAGCTTTATCTGGAAAATATAGACGAGTTCGTCACGGACC and reverse primer CACGTGGACCGGTGAATTCGGCTATTATTTCCTCTGGAAGAAGCCAG. A 144-amino-acid N-terminal p66 fragment ($p66_N$) was cloned by PCR to pFastBac1 transfer vector using the forward primer AGCTTCGGATCCTAAATATGGCGGACCAGCTTTATCTGG, the reverse primer AGATGAATTCTCAAGCTCTAGGGACGGCAGCTG and *Bam*HI/*Eco*RI restriction sites. The p50 subunit with an N-terminal His tag (p50) was cloned by PCR to the pFastBac1 transfer vector using the forward primer CGTATGGATCCAATATGGGTCATCATCATCATCATCATGGAATGTTTTCTGAGCAGGCTGCC, the reverse primer GGACGTCAGTGAATTCAGGTTATCAGGGGCCCAGCC and *Bam*HI/*Eco*RI restriction sites. High-titer viruses for the p50 and $p66_N$ subunits were obtained using the Bac-to-Bac Baculovirus Expression System from Invitrogen. $1.8 \times 10^9$ Sf21 cells in 1 l shaking culture were infected simultaneously with p50 and $p66_N$ recombinant viruses at a multiplicity of infection of 1:3 and were cultivated at 300 K for 56 h. Cells were harvested by centrifugation at 160*g* for 5 min and frozen. The cell pellet (15 ml) was defrosted on ice and lysed in 120 ml buffer *A* [20 m*M* Tris–HCl pH 7.8, 0.1 *M* NaCl, 1 m*M* imidazole–HCl, 2 m*M* $K_2HPO_4$, 5% glycerol, 5 m*M* $\beta$-mercaptoethanol ($\beta$-ME), 0.5 m*M* PMSF and 1 mg $l^{-1}$ leupeptin]. Cell debris was removed by centrifugation and the obtained lysate was clarified by 0.05% polyethyleneimine precipitation, passed through a 0.2 µm filter and loaded onto a 15 ml Profinity IMAC resin column (Bio-Rad) charged with $NiCl_2$. The column was washed with 150 ml buffer *A* containing 150 m*M* NaCl and the p50–$p66_N$ dimer was eluted with a 150 ml gradient of 0.12 *M* imidazole–HCl pH 7.7 in buffer *A*. Next, the dimer was loaded onto 7 ml hydroxyapatite Bio-Gel HT resin (Bio-Rad); the column was washed with 21 ml buffer *A* and equilibrated with buffer *B* (20 m*M* Tris–HCl pH 7.8, 10 m*M* NaCl, 2 m*M* $K_2HPO_4$, 5 m*M* $\beta$-ME). The dimer was eluted with a 35 ml gradient of 50 m*M* $K_2HPO_4$ in buffer *B*. The eluate obtained from the hydroxyapatite column (20 ml; 14 mg protein by Bradford assay) was dialyzed overnight into 0.6 l 10 m*M* Tris–HCl pH 7.8, 5 m*M* EDTA, 1 m*M* DL-dithiothreitol (DTT) and then in 4 h into 0.6 l 7 m*M* Tris–HCl pH 7.8, 2 m*M* DTT. The purified dimer was concentrated to 12 mg $ml^{-1}$ and frozen. The final product was of high purity (Fig. 1*a*).

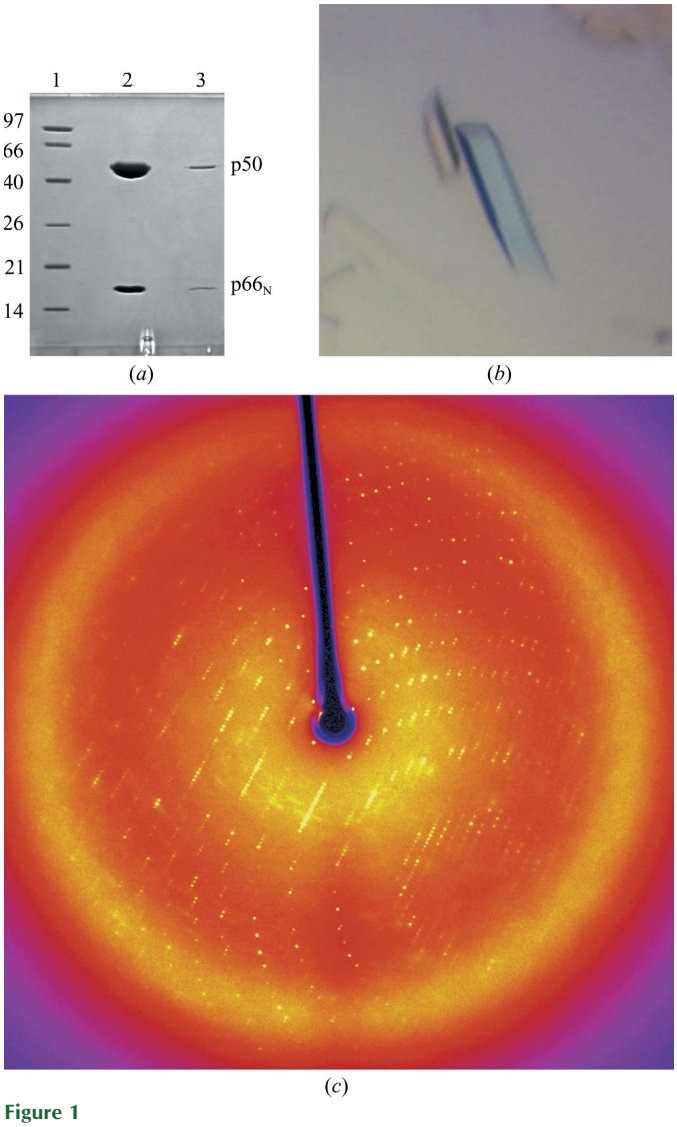


**Figure 1**
$p50–p66_N$ sample and crystal. (*a*) 13% SDS–PAGE. Lane 1, molecular-weight markers (kDa). Lane 2, analysis of the initial sample. Lane 3, washed and dissolved crystal content. (*b*) A photomicrograph of a crystal. (*c*) The X-ray diffraction pattern of the crystal shown in (*b*) recorded on an R-AXIS IV imaging plate; the oscillation angle was 1.0°, the exposure time was 20 min, the radiation was Cu $K\alpha$ and the crystal-to-imaging plate distance was 240 mm.

### 2.2. Crystallization

Initial crystallization conditions were obtained by screening at 298 K in 96-well plates using the sitting-drop vapor-diffusion method with Crystal Screens I and II (Hampton Research; Jancarik & Kim, 1991; Cudney *et al.*, 1994) and 50% diluted solutions of Crystal Screens I and II. Drops consisting of 1 µl protein solution mixed with 1 µl reservoir solution were equilibrated against 100 µl reservoir solution. The screens were also performed with reservoir solutions containing 20 m*M* DTT. Several conditions from the 50% diluted and DTT-containing screen produced tiny needle-like crystals. Based on the conditions producing these crystals, grid screens with variations in precipitant concentration, salt type and concentration and pH were prepared and tested. After improvement using the grid screens, the shape of the crystals was clearly identifiable as a prism with a rhombic cross-section; however, the crystals were still tiny. The best condition was used for further screening with Hampton Research Additive Screen by mixing 10% of a screen solution with reservoir solution in each well. The addition of EDTA sodium salt dramatically improved the size of the crystals. The largest crystals grew to dimensions of $1.0 \times 0.3 \times 0.1$ mm in two to three weeks using a reservoir solution containing 50 m*M* imidazole pH 6.5, 300 m*M* sodium acetate, 20 m*M* DTT, 10 m*M* EDTA sodium salt and 3%(*w*/*v*) PEG 1000. The highest resolution from these highly anisotropically diffracting crystals was limited to 3.5 Å. Further modification of the crystallization conditions [100 m*M* imidazole pH 6.5, 450 m*M* sodium acetate, 5 m*M* tris-(2-carboxyethyl)phosphine hydrochloride (TCEP) and 1%(*v*/*v*) glycerol] yielded crystals of the same shape and unit-cell parameters but smaller size ($0.45 \times 0.15 \times 0.05$ mm; Fig. 1*b*). Importantly, these crystals exhibited significantly reduced anisotropy and diffracted to at least 3 Å resolution (Fig. 1*c*).

### 2.3. Data collection

For data collection, the crystals were soaked in cryoprotectant for a few seconds, mounted in nylon-fiber loops and flash-cooled in a dry nitrogen stream at 100 K. The cryoprotectant was prepared by adding 35%(*v*/*v*) ethylene glycol to the reservoir solution and increasing the concentration of sodium acetate to 0.5 *M*. A complete diffraction

**Table 1**
Crystal parameters and data-collection statistics.

Values in parentheses are for the last shell.

| | |
|---|---|
| Crystal parameters | |
| Unit-cell parameters | |
| $a$ (Å) | 95.13 |
| $b$ (Å) | 248.54 |
| $c$ (Å) | 103.46 |
| $\beta$ (°) | 106.94 |
| Space group | $P2_1$ |
| Data collection | |
| Temperature (K) | 100 |
| Resolution (Å) | 40–3.0 (3.11–3.0) |
| Unique reflections | 85645 |
| Redundancy | 2.6 (2.1) |
| Completeness (%) | 93.0 (90.4) |
| $R_{\rm merge}$† (%) | 7.9 (43.0) |
| $\langle I/\sigma(I)\rangle$ | 21.2 (3.8) |
| Mosaicity (°) | 0.53–0.84 |

† $R_{\rm merge} = \sum_{hkl}\sum_i |I_i(hkl) - \langle I(hkl)\rangle| / \sum_{hkl}\sum_i I_i(hkl)$, where $I_i(hkl)$ and $\langle I(hkl)\rangle$ are the intensity of measurement $i$ and the mean intensity for the reflection with indices $hkl$, respectively.

data set was collected at cryotemperature on a Rigaku R-AXIS IV imaging plate using Osmic VariMax HR mirror-focused Cu $K\alpha$ radiation from a Rigaku FR-E rotating-anode generator operated at 45 kV and 45 mA. The exposure time and oscillation angle per image were 20 min and 1°, respectively. All intensity data were indexed, integrated and scaled with *DENZO* and *SCALEPACK* from the *HKL*-2000 program package (Otwinowski, 1993; Otwinowski & Minor, 1997). The crystal parameters and data-processing statistics are summarized in Table 1.

## 3. Results and discussion

Protein expression, purification, concentration and storage protocols were optimized to obtain high-purity monodisperse and reproducible samples of p50–p66$_{\rm N}$. Samples that were stored at 253 or 193 K and thawed before use were similar to freshly prepared samples. The quality of the samples was monitored using both SDS–PAGE analysis and dynamic light-scattering (DLS) measurements. The polydispersity of the best sample was 14% and the molecular weight corresponded to a single heterodimer. The preparation of a monodisperse p50–p66$_{\rm N}$ sample and the addition of reducing reagents (DTT and/or TCEP) were critical for the success of initial crystallization screens. We also attempted to purify the p50 and p66$_{\rm N}$ subunits separately after expression in Sf21 insect cells infected with the respective baculoviruses. p66$_{\rm N}$ was expressed as an insoluble protein. We were able to obtain high-purity p50 subunit with a high yield, but we could not overcome its tendency to aggregate at concentrations over 1 mg ml$^{-1}$.

Optimization of crystal-producing conditions with fine screens finally produced p50–p66$_{\rm N}$ crystals which diffracted to 3 Å resolution (Fig. 1*c*) and were suitable for detailed structural study. The crystal was monoclinic, belonging to space group $P2_1$. A solvent-content calculation (Matthews, 1968) suggested that four molecules of p50–p66$_{\rm N}$ were located in the asymmetric unit, assuming the solvent content of the crystal to be 72.2%. A search for closely related structures in the PDB using the p50 and p66$_{\rm N}$ amino-acid sequences did not reveal a suitable hit for use as a search model in the molecular-replacement method. Therefore, the structure will be determined using the multiple isomorphous replacement method.

We thank J. Lovelace and G. E. Borgstahl for maintenance and management of the Eppley Institute's X-ray Crystallography facility and O. Baranovskaya for making the full-length p66 cDNA and cloning it into pFastBac1 transfer vector. The primers were synthesized in the Eppley Institute's Molecular Biology Core facility. Both facilities are supported by the Cancer Center Support Grant P30CA036727. This work was supported in part by the UNMC Eppley Cancer Center Pilot Project LB595 to THT.

## References

Cudney, R., Patel, S., Weisgraber, K., Newhouse, Y. & McPherson, A. (1994). *Acta Cryst.* D**50**, 414–423.
Gerik, K. J., Li, X., Pautz, A. & Burgers, P. M. (1998). *J. Biol. Chem.* **273**, 19747–19755.
Gibbs, P. E., McDonald, J., Woodgate, R. & Lawrence, C. W. (2005). *Genetics*, **169**, 575–582.
He, H., Tan, C. K., Downey, K. M. & So, A. G. (2001). *Proc. Natl Acad. Sci. USA*, **98**, 11979–11984.
Huang, M. E., de Calignon, A., Nicolas, A. & Galibert, F. (2000). *Curr. Genet.* **38**, 178–187.
Huang, M. E., Rio, A. G., Galibert, M. D. & Galibert, F. (2002). *Genetics*, **160**, 1409–1422.
Jancarik, J. & Kim, S.-H. (1991). *J. Appl. Cryst.* **24**, 409–411.
Johansson, E., Garg, P. & Burgers, P. M. (2004). *J. Biol. Chem.* **279**, 1907–1915.
Li, H., Xie, B., Rahmeh, A., Zhou, Y. & Lee, M. Y. (2006). *Cell Cycle*, **5**, 428–436.
Li, H., Xie, B., Zhou, Y., Rahmeh, A., Trusa, S., Zhang, S., Gao, Y., Lee, E. Y. & Lee, M. Y. (2006). *J. Biol. Chem.* **281**, 14748–14755.
Liu, L., Mo, J., Rodriguez-Belmonte, E. M. & Lee, M. Y. (2000). *J. Biol. Chem.* **275**, 18739–18744.
Liu, L., Rodriguez-Belmonte, E. M., Mazloum, N., Xie, B. & Lee, M. Y. (2003). *J. Biol. Chem.* **278**, 10041–10047.
Lydeard, J. R., Jain, S., Yamaguchi, M. & Haber, J. E. (2007). *Nature (London)*, **448**, 820–824.
McCulloch, S. D. & Kunkel, T. A. (2008). *Cell Res.* **18**, 148–161.
Matthews, B. W. (1968). *J. Mol. Biol.* **28**, 491–497.
Otwinowski, Z. (1993). *Proceedings of the CCP4 Study Weekend. Data Collection and Processing*, edited by L. Sawyer, N. Isaacs & S. Bailey, pp. 56–62. Warrington: Daresbury Laboratory.
Otwinowski, Z. & Minor, W. (1997). *Methods Enzymol.* **276**, 307–326.
Pavlov, Y. I., Shcherbakova, P. V. & Rogozin, I. B. (2006). *Int. Rev. Cytol.* **255**, 41–132.
Podust, V. N., Chang, L. S., Ott, R., Dianov, G. L. & Fanning, E. (2002). *J. Biol. Chem.* **277**, 3894–3901.
Pohler, J. R. G., Otterlei, M. & Warbrick, E. (2005). *BMC Mol. Biol.* **6**, 17.
Szekely, A. M., Chen, Y. H., Zhang, C., Oshima, J. & Weissman, S. M. (2000). *Proc. Natl Acad. Sci. USA*, **97**, 11365–11370.